Formation of the Meta II Photointermediate Is Accompanied by Conformational Changes in the Cytoplasmic Surface of Rhodopsin†

John F. Resek,‡ Zohreh Toossi Farahbakhsh,§ Wayne L. Hubbell,§ and H. Gobind Khorana*,‡

Departments of Biology and Chemistry, Massachusetts Institute of Technology, 77 Massachusetts Avenue, Cambridge, Massachusetts 02139, and Jules Stein Eye Institute, Department of Chemistry and Biochemistry, University of California, Los Angeles, California 90024-7008

Received July 6, 1993; Revised Manuscript Received August 31, 1993®

ABSTRACT: Five mutations of rhodopsin have been produced, each of which contains a unique cysteine residue at positions 62, 65, 140, 240, or 316 in the cytoplasmic domain. The single reactive cysteines were derivatized with a sulfhydryl-specific nitroxide spin-label, and the electron paramagnetic resonance (EPR) spectra were analyzed in both lauryl maltoside and digitonin in the dark and after photobleaching. The collision rate of the attached nitroxides with polar and nonpolar paramagnetic agents indicated that they were all exposed to the aqueous environment. Photobleaching of the mutants in digitonin, which arrests the protein at the meta I intermediate, produced little change in mobility of the attached nitroxide. On the other hand, photobleaching in lauryl maltoside produced the meta II intermediate and significant changes in the EPR spectra of the nitroxides attached to positions 140 and 316. These data directly reveal a light-induced conformational change in the cytoplasmic loops that accompanies meta II formation.

Rhodopsin, the membrane-bound photoreceptor in the vertebrate rod cell, contains 1 polypeptide chain of 348 amino acids whose sequence has been determined by cDNA and protein sequencing (Ovchinnikov *et al.*, 1982; Hargrave *et al.*, 1983; Nathans & Hogness, 1983). A secondary structure model, assuming that the protein contains seven transmembrane helices, is shown in Figure 1. The chromophore 11-*cis*-retinal, located in the membrane-embedded helical cluster, is linked to Lys296 in helix G via a protonated Schiff base. Glutamic acid 113, in helix C, serves as the counterion to the retinylidene Schiff base placing helix C and G in apposition to each other (Sakmar *et al.*, 1989; Zhokovsky & Oprian, 1989; Nathans, 1990). The cytoplasmic interhelical loops (C→D, E→F, and G→carboxyl terminus) contain the light-dependent binding site for transducin (Konig *et al.*, 1989a; Franke *et al.*, 1990, 1992) (G_t)[1] whereas the carboxyl tail contains the sites for light-dependent phosphorylation (Kuhn, 1984).

Upon absorption of a photon, 11-*cis*-retinal undergoes isomerization to the *all-trans* form ("bleaching"), which triggers the formation of several photointermediates (Wald, 1968): rho (500 nm) → batho (548 nm) → lumi (497 nm) → meta I (480 nm) → meta II (380 nm) → meta III (450 nm) → opsin + free retinal (380 nm). One of these intermediates, rhodopsin meta II, binds to and activates G_t (Emeis *et al.*, 1982). This represents the first step in a cascade which leads to hyperpolarization of the rod cell.

One approach to studying structural changes in rhodopsin induced by bleaching is to introduce cysteine residues at suitable sites and then derivatize them with the sulfhydryl-specific spin-labeling reagent proxylmethanethiosulfonate (I) (Altenbach *et al.*, 1990; Greenhalgh *et al.*, 1992). An analysis

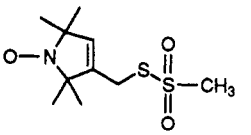

(I)

of the EPR line shape of the attached nitroxide and its collision rate with paramagnetic reagents in solution can give insights regarding local structure as well as the location of the spin-labeled residues relative to the hydrophobic/hydrophilic boundaries in rhodopsin. Most importantly for the present work, the EPR spectra are highly sensitive to changes in local conformation.

Five mutants with a unique derivatizable cysteine residue at positions 62, 65, 140, 240, or 316 on the cytoplasmic surface of rhodopsin have been constructed and used to site-direct the spin-labeling reagent. The EPR spectra of the labeled mutants in lauryl maltoside and digitonin were analyzed in terms of both structure and conformational changes induced by bleaching. The results show that the attached labels all lie in the aqueous phase, supporting the model in Figure 1. An important conclusion is that light-induced conformational changes are located at positions 140 and 316, near the cytoplasmic terminations of helices C and G, respectively, only upon formation of the active meta II intermediate. These data are consistent with earlier studies indicating that the formation of the meta II species corresponds to activation of the visual cascade (Wald, 1968; Emeis *et al.*, 1982).

† This work was supported by National Institutes of Health Grants GM 28289 and AI 11479 (to H.G.K.), NIH Fellowship EYO6189 (to J.F.R.), NIH Grant EYO5216 (to W.L.H.), NIH Trianing Grant EYO7026 (to Z.T.F.) and a Jules Stein Professorship endowment (to W.L.H.). This paper was the result of an equal contribution from both J.F.R. and Z.T.F.

* Address correspondence to this author.
‡ Massachusetts Institute of Technology.
§ University of California, Los Angeles.

® Abstract published in *Advance ACS Abstracts,* October 15, 1993.

[1] Abbreviations: G_t, transducin; GTPγS, guanosine 5′-*O*-(3-thiotriphosphate); GMPPNP, guanylyl imidodiphosphate; EPR, electron paramagnetic resonance; MES, sodium 2-(*N*-morpholino)ethanesulfonic acid; LGR, loop–gap resonator; Crox, chromium oxalate; $Ni(AA)_2$, nickel acetylacetonate; UV, ultraviolet; vis, visible; WT, wild type; T_α, α-transducin.

0006-2960/93/0432-12025$04.00/0

EXPERIMENTAL PROCEDURES

Materials

Restriction endonucleases, GMPPNP, and GTPγS were from Boehringer Mannheim Biochemicals (Indianapolis, IN). Frozen retinas were purchased from J. A. Lawson Co. (Lincoln, NE). Lauryl maltoside was purchased from Anatrace (Maumee, OH) and digitonin from Calbiochem (San Diego, CA). [^{35}S]GTPγS (1400 Ci/mmol) was from DuPont—New England Nuclear (Boston, MA). ConA–Sepharose was purchased from Pharmacia (Piscataway, NJ). Proxyl-methanethiosulfonate (I) was obtained from Reanal (Budapest, Hungary).

Methods

Construction of Mutant Rhodopsin Genes. Oligonucleotides were synthesized using an Applied Biosystems 380A DNA synthesizer, purified by denaturing acrylamide electrophoresis, and characterized by 5′-end nucleotide analysis (Ferretti *et al.*, 1986). The oligonucleotides were used to construct six mutant rhodopsin genes by restriction fragment replacement in the synthetic rhodopsin gene contained within the pTN2 cloning vector (Ferretti *et al.*, 1986; Nakayama & Khorana, 1991). The base mutant φ (Cys140,316,322, 323→Ser) was constructed by replacing the *Pvu*I–*Sfi*I gene fragment (bp 400–514) with two synthetic duplexes containing a Cys140→Ser codon substitution. The *Nde*I–*Not*I fragment (bp 808–1059) was then replaced with the same gene fragment from Cys*X* which contained the codon substitutions for Cys316,322,323→Ser. The mutant C140 gene was constructed by placing the Cys*X*, *Nde*I–*Not*I fragment into the WT gene. Additional mutants were constructed from the φ gene by a two-part ligation. The mutant C316 was constructed by ligating the *Eco*RI–*Bst*E2 fragment (bp 1–963) from the Cys140→Ser gene with the φ gene. Replacements for Thr62 and His65 were made by two-part ligations of the *Bcl*I–*Hin*dIII vector fragment (bp 146–211) with synthetic duplexes containing the nucleotide replacement. The Ser240 replacement was made by a two-part ligation with the *Pst*I–*Dde*I (bp 704–739) vector fragment and a synthetic duplex containing the cysteine codon substitution. The mutant constructs were transferred to the pMT3 vector for expression in COS-1 cells (Oprian *et al.*, 1987).

Expression, Purification, and Characterization of Mutant Rhodopsins. The opsin genes were transiently expressed in COS-1 cells as described (Oprian *et al.*, 1987). The rhodopsin chromophore was generated by adding 11-*cis*-retinal (5 μM) to a cell suspension in the dark. Cells were solubilized in 1% lauryl maltoside and the rhodopsin mutants purified by immunoaffinity chromatography (Franke *et al.*, 1992).

Purified rhodopsin mutants were characterized in three ways: (a) UV–vis spectroscopy; (b) SDS–PAGE followed by visualization of the protein by a Western blot using the 1D4 monoclonal antibody (Molday & Mackenzie, 1983); and (c) a transducin activation assay as described below.

Transducin was purified by the methods previously described (Baehr *et al.*, 1982). The ability of the mutants to activate transducin was determined by binding of [^{35}S]GTPγS (Wessling-Resnick & Johnson, 1987). Briefly, bovine or COS cell rhodopsin (5 nM) was incubated in the presence of transducin (500 nM) and [^{35}S]GTPγS (1 μM) in 100 μL of a buffer containing 0.02% lauryl maltoside, 5 mM MES, pH 6.0, 100 mM NaCl, and 5 mM $MgCl_2$. Samples were incubated for 90 min at 4 °C in the dark or under constant illumination with a λ >495-nm long-pass filter. Following the incubation, the samples were diluted with 10 mL of an ice-cold buffer containing 5 mM MES, pH 6.0, and 5 mM $MgCl_2$ and filtered through nitrocellulose. The filter was washed twice with 5 mL of buffer and the radioactive content determined with an LKB 1209 Rackbeta liquid scintillation counter.

Derivatization of Mutants with Spin-Label. Mutants expressed in COS cells were derivatized while bound to 1D4–Sepharose. Three hundred microliters of 1D4 resin with bound COS cell rhodopsin was incubated in 3 mL of the buffer containing 5 mM MES, pH 6.0, 0.02% lauryl maltoside, and 100 μM methanethiosulfonate spin-label (I) for 3 h at room temperature with gentle agitation. After incubation, the supernatant was removed, the resin was washed 5 times with 10 mL of a buffer containing 0.02% lauryl maltoside and 5 mM MES, pH 6.0, and rhodopsin was eluted as previously described (Franke *et al.*, 1992).

EPR Spectroscopy. Due to the small quantities of mutant protein (5–20 μg), it was essential to use the loop–gap resonator (LGR) previously described (Hubbell *et al.*, 1987). The LGR used has an active volume of about 1.2 μL. Solutions of the labeled mutants in either digitonin or lauryl maltoside (5–10 μg/mL) were concentrated to a volume of 5–10 μL using centrifugal filtration units (Millipore Ultrafree-MC, 10 000 MW cutoff). Due to the very small volumes and variable loss on the filters, it was not possible to accurately control the final concentration, which varied from sample to sample.

Signal-averaged EPR spectra were recorded at 2-mW incident microwave power under field/frequency lock on a Varian E-109 X-band spectrometer modified for the LGR as previously described (Hubbell *et al.*, 1987). Typically, 8–16 scans were required.

To estimate the number of spin-labels per rhodopsin, the EPR spectra were double-integrated, and the area was compared with that of a known standard. These determinations were done only in lauryl maltoside, where the final signal-to-noise ratio was relatively high. Estimated random error in the integration based on repetitive integrations of the same sample was typically <5%. Other sources of error such as non-zero base-line values accumulated during signal averaging are difficult to estimate, but integrals obtained with nonlabeled samples were zero within the error estimated above. The rhodopsin content of the same samples was estimated after dilution in lauryl maltoside from the optical density at 500 nm, using an extinction coefficient of 42 700 cm^{-1} M^{-1}. The maximum error in this determination was estimated to be ±15% based on two independent determinations in each case.

Collision frequencies with diffusible paramagnetic reagents and the corresponding Π values were estimated by continuous-wave power saturation techniques as previously described (Altenbach *et al.*, 1989; Farahbakhsh *et al.*, 1992).

Photolysis of labeled rhodopsin was carried out using a 75-W quartz–iodide source fitted with a heat filter and a long-wavelength pass filter (Melles-Griot, λ >500 nm). For digitonin solutions, photolysis was carried out at 4 °C for 3 min, the sample was warmed to ambient temperature (22 °C), and the spectra were immediately recorded. For lauryl maltoside solutions, photolysis at ambient temperature or 4 °C produced equivalent results, and was carried out routinely at ambient temperature.

Purification of Bovine Rhodopsin. ROS membranes were prepared as described previously (Papermaster, 1982) and stored frozen in the dark at −79 °C under argon. To purify rhodopsin, ROS membranes (500 μg of protein) were thawed

Table I: Characterization of Rhodopsin Cysteine Mutants[a]

mutant	native cysteines changed to serine	loop	yield (μg)	λ_{max} (nm)	A_{280}/A_{500}	GDP/GTPγS exchange (pmol)	
						hν	d*k*
WT			13	500	1.66	14.5 ± 0.6	1.1 ± 0.1
φ	140, 316, 322, 323		9	499	1.63	14.9 ± 0.3	1.4 ± 0.7
C140	316, 322, 323	C–D	10	500	1.70	16.9 ± 0.4	1.2 ± 0.1
C316	140, 322, 323	G-tail	10	499	1.71	15.4 ± 0.3	1.2 ± 0.2
T62C	140, 316, 322, 323	A–B	2.5	494	1.85	15.4 ± 0.3	1.5 ± 0.1
H65C	140, 316, 322, 323	A–B	10	499	1.65	15.9 ± 0.1	1.9 ± 0.3
S240C	140, 316, 322, 323	E–F	8	503	1.78	12.7 ± 0.7	1.9 ± 0.3

[a] The amino acid replacements to each mutant are shown along with the yield in micrograms of protein per 14-cm Nunc Plate. The λ_{max} and A_{280}/A_{500} ratio were similar to those for the WT protein for each of the mutants. The GDP/GTPγS column gives the picomoles of GTPγS retained on a nitrocellulose filter from equilibrium binding assays. GTPγS binding was determined from three separate observations.

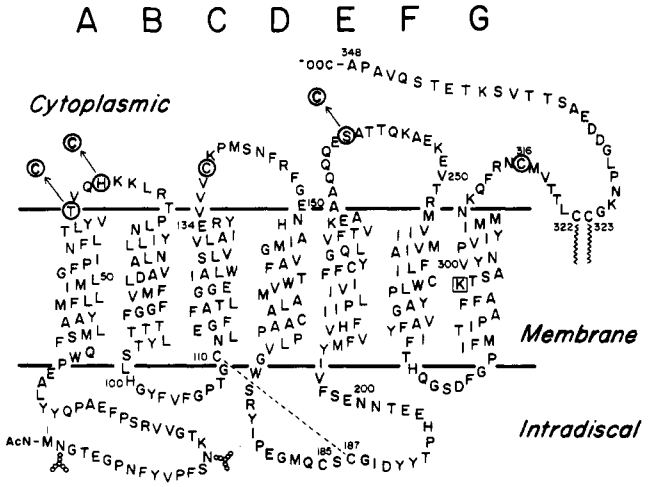

FIGURE 1: Secondary structural model of bovine rhodopsin. Single-letter abbreviations are used for amino acids. The circled amino acids indicate the positions of the cysteine replacements. The dashed line between Cys110 and Cys187 on the intradiscal side shows a disulfide bond. Cys322 and Cys323 on the cytoplasmic face are palmitoylated in the WT protein. In the base mutant, φ, residues Cys140, -316, -322, and -323 were replaced with serine. The mutant φ was then used for the construction of five additional mutants with cysteines at position 62, 65, 140, 240, or 316.

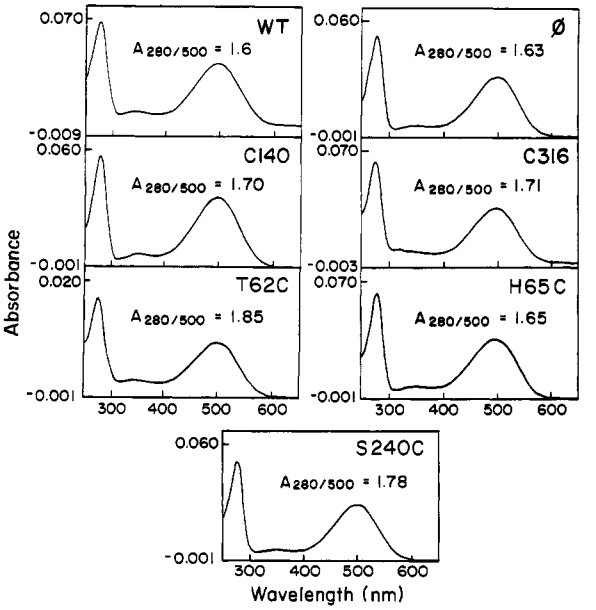

FIGURE 2: UV–vis spectra of COS cell rhodopsin mutants purified by immunoaffinity chromatography. The $A_{280/500}$ spectral ratio was between 1.6 and 1.85, indicating that each of the mutant proteins was essentially pure.

in the dark in 1 mL of 1% of a detergent solution (either lauryl maltoside or digitonin) containing 10 mM HEPES, pH 7.5, 1 mM $MgCl_2$, and 1 mM $CaCl_2$. A 100-μL aliquot of ConA–Sepharose was then added, and the solution was mixed gently. After 1 h, the Sepharose beads were pelleted by centrifugation and washed 6 times with 1.5 mL of buffer containing 0.05% detergent, 10 mM HEPES, and 5 mM $MgCl_2$. Rhodopsin was then eluted in 300 μL of the same buffer containing 200 mM methyl α-mannoside 2 times. Prior to obtaining UV–vis spectra, the sample was centrifuged at 50 000 rpm (Beckman TL-100 rotor) for 30 min to remove any particulate substances from the supernatant. Approximately 50% of the bovine rhodopsin was recovered with 280/500-nm ratios of 1.8. Bleaching studies were performed with a Dolan-Jenner fiber optic lamp filtered through a 495-nm long-pass filter in the presence or absence of 1 μM transducin. UV–vis spectra were obtained on a Perkin Elmer λ-7 spectrophotometer.

RESULTS

Construction of Rhodopsin Mutants. Mutants with single reactive cysteines were constructed from a base mutant, φ, in which Cys140, -316, -322, and -323 were replaced by serine. Previous work has established that Cys140 and Cys316 are the only two cysteines in rhodopsin that react with sulfhydryl reagents in the dark (Findlay *et al.*, 1982). Since recent results suggest that replacements made at position 140 result in the palmitoylated residues Cys322 and -323 becoming available for derivatization, these were also replaced with serine (Karnik *et al.*, 1993). Cysteine replacements were then introduced into φ at positions 140, 316, 62, 65, or 240 for selective derivatization with the spin-label I. The location of these cysteines is shown in Figure 1. The amino acid substitutions made in each mutant are summarized in Table I.

Characterization of Cysteine Mutants. (A) UV–vis Spectra. The characterization of the purified COS cell mutants is summarized in Table I. All the mutants bound 11-*cis*-retinal to form a chromophore with an absorption maximum near 500 nm. Derivatization with spin-label I did not significantly alter the visible absorption spectrum. As shown in Figure 2, the 280/500-nm absorbance ratio for each mutant was between 1.6 and 1.8, indicating that the protein preparation was pure. Most of the constructs produced 65–85% of the WT yields, although the mutant C62 gave only 20% of the WT yields.

(B) 1D4 Western Blot of the Rhodopsin Cysteine Mutants. Figure 3 shows a Western blot of bovine and COS-1 cell rhodopsins using the 1D4 anti-rhodopsin antibody. The WT protein expressed in COS cells has a major 41-kDa polypeptide and several higher molecular weight species. The glycosylated species collapse to a single 31-kDa protein following Endo F treatment (Karnik *et al.*, 1988). Each of the mutants expressed in COS cells had the same glycosylation pattern seen for the

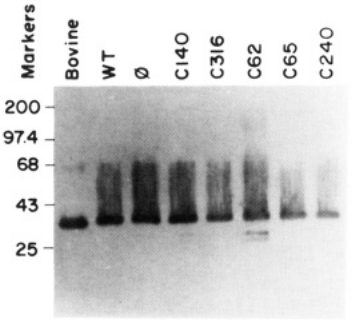

FIGURE 3: Immunoblot analysis of 1D4-purified rhodopsin, cysteine mutants, and bovine rhodopsin. The samples (200 ng) were subjected to SDS–PAGE and a 1D4 immunoblot. Each of the mutants shows the same glycosylation pattern seen in the WT protein. The low molecular weight band present in the case of C62 represents a minor amount of unglycosylated rhodopsin.

Table II: Quantitation and Accessibility of Cysteine Mutants to O_2, Crox, and $Ni(AA)_2$

rhodopsin	mol of nitroxide/ mol of protein[a]	collision parameter, Π[b]		
		Π(O_2)	Π(Crox)	Π[$Ni(AA)_2$]
bovine	2.3			
WT	2.3			
ϕ	0.3			
C140	1.6	0.7	0.2	0.3
C316	1.3	0.7	0.3	0.3
C62	2.0	0.4	0.3	0.1
C65	1.4	0.9	0.5	0.3
C240	1.4	1.5	1.4	2.2

[a] Error estimated to be ca. 20%. [b] Error estimated to be ca. 10%. Π(Crox) and Π[$Ni(AA)_2$] were determined in the presence of 20 mM of the respective reagents, and Π(O_2) was determined in equilibrium with air.

WT protein. The heterogeneous pattern of glycosylation indicates that the mutant rhodopsins were properly folded and transported to the cytoplasmic membrane. The Western blot for C62 reveals lower molecular weight bands in addition to the WT glycosylated species. These represent a small fraction of partially glycosylated rhodopsin.

(*C*) *Transducin Activation.* Bleached rhodopsin catalyzes the exchange of GTP/GDP on the α-subunit of transducin (Fung *et al.*, 1981). This was monitored by the exchange of GDP for [^{35}S]GTPγS on T_α (Wessling-Resnick & Johnson, 1987). The results shown in Table I indicate that each of the mutants can stimulate GTPγS exchange in a light dependent-manner.

EPR Analysis. (*A*) *Quantitation of the Nitroxide Spin-Label.* Rhodopsin, either native or COS cell-expressed, was derivatized with the spin-label I, and the moles of nitroxide per mole of protein was estimated. The results are presented in Table II. Both native and WT rhodopsin from COS cells had 2.3 ± 0.4 mol of nitroxide/mol of protein while ϕ contained 0.3 ± 0.4 mol of nitroxide/mol of protein. The small amount of reactivity in this mutant is presumably due to a limited reaction with buried cysteines 222 and/or 167. Each of the cysteine mutants except C62 had approximately 1 mol of nitroxide/mol of protein in addition to the background labeling level.

(*B*) *Topographical Location of the Spin-Labeled Cysteine.* To determine the topographical location of the spin-labeled site in the molecule, the accessibility of the nitroxide to collision with O_2, chromium(III) oxalate (Crox), and nickel(II) acetylacetonate [$Ni(AA)_2$] was investigated for each of the spin-labeled mutants, and the data were expressed in terms of the dimensionless parameter Π, a quantity proportional to

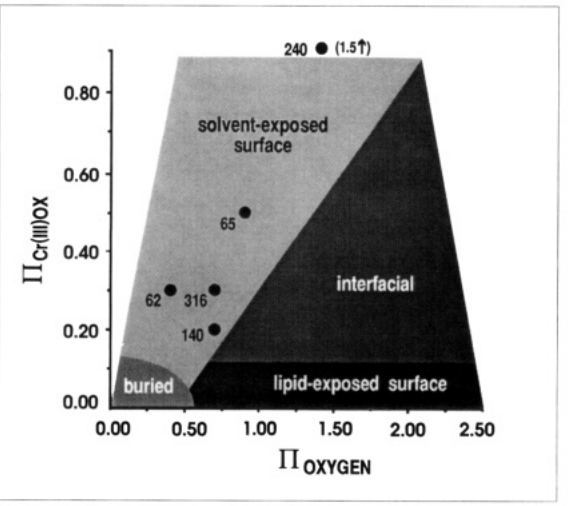

FIGURE 4: Plot of Π(O_2) *versus* Π(Crox) for spin-label I attached to the various cysteine mutants indicated. The shaded areas defining the topological domains were constructed according to data from spin-labeled bacteriorhodopsin mutants (see text).

the collision rate and independent of instrumental parameters (Farahbakhsh *et al.*, 1992). Interpretation of data of this type in terms of the molecular topography for membrane proteins requires at least two dimensions of Π: one for collision with a hydrophobic radical, such as O_2, and the other for collision with a hydrophilic radical, such as Crox or $Ni(AA)_2$. Two dimensions are sufficient to resolve solvent-exposed, lipid-exposed, and buried sites (Hubbell & Altenbach, 1993). A plot of Π(O_2) *versus* Π(Crox) for the rhodopsin mutants in lauryl maltoside is shown in Figure 4 (solid points). The approximate boundaries shown for buried, solvent-exposed, and lipid-exposed domains were determined from previously reported data (Altenbach *et al.*, 1989; Greenhalgh *et al.*, 1992) on bacteriorhodopsin from spin-labeled sites known to occupy those domains (Henderson *et al.*, 1990).

With this calibration, the cysteine residues 62, 65, 140, and 316 in rhodopsin are at solvent-exposed sites, consistent with their placement in interhelical loops as shown in the secondary structural model of Figure 1. Cysteine 240 is particularly interesting, since it has much larger Π values than any of the others; i.e., it experiences much higher collision rates with diffusible radicals in solution. In fact, the Π values lie near the maximum observable for a nitroxide in water at the concentrations of O_2 and Crox used. This implies that there are few local steric constraints around the nitroxide, suggesting an unstructured, mobile domain. This conclusion is consistent with the EPR line shape of the nitroxide at C240, which indicates an unusually high degree of motion for I attached to a cysteine in a protein (Figure 5).

Crox is a negatively charged complex, and the concentration in the vicinity of the nitroxide, and hence the collision frequency with the nitroxide, will be influenced by the local electrostatic potential. To examine the role of electrostatic interactions, Π[$Ni(AA)_2$] was also determined for the labeled mutants (Table II). $Ni(AA)_2$ is a neutral complex of similar size to Crox whose collision rate is unaffected by electrostatic potentials. As for Crox, the collision rate for C240 is much higher than for the other positions, indicating that the effect is indeed due to a lack of steric hindrance and not to electrostatic interactions. For C316, the results are identical, within experimental error, to Crox. At C62 and C65, Π-[$Ni(AA)_2$] is significantly smaller than Π(Crox), suggesting the possibility of a positive electrostatic potential near these sites due to charges on the protein. Despite these individual

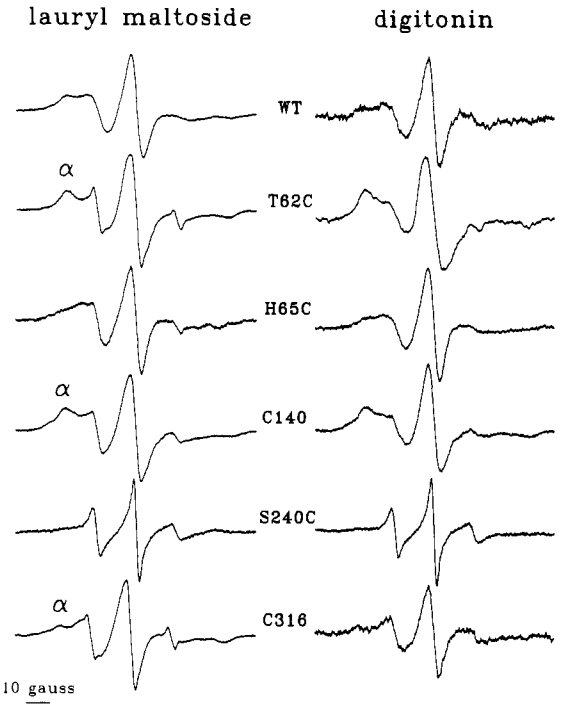

FIGURE 5: EPR spectra for spin-labeled COS cell rhodopsin and mutants in lauryl maltoside and digitonin. The spectra were recorded under dim red light at ambient temperature. A resolved spectral component corresponding to a relatively immobilized spin population is identified as α.

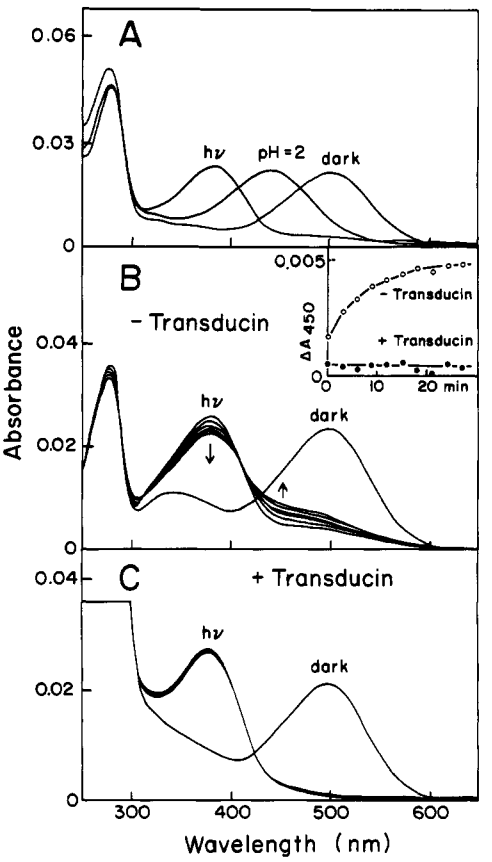

FIGURE 6: Bleaching of bovine rhodopsin in lauryl maltoside. (A) Rhodopsin solubilized in lauryl maltoside produces meta II when bleached. Reducing the pH to 2 results in denaturation of rhodopsin and formation of a protonated Schiff base (λ_{max} = 440 nm). (B) At 20 °C, there is a slow decay of the meta II species to meta III (λ_{max} = 450 nm). (C) In the presence of transducin, meta II is stabilized, and meta III formation is inhibited. (B inset) The rise at 450 nm, relative to the meta II–meta III isosbestic point, is shown in the absence (○) or the presence (●) of transducin.

variations, the Π[Ni(AA)$_2$] values for the various mutants fall within the topological domains assigned by the Crox values, and further support the assignment.

The EPR spectra for the labeled mutants in lauryl maltoside and digitonin in the dark are shown in Figure 5. The spectra generally reflect a distribution of motional states, characteristic of other spin-labeled proteins (Ogawa & McConnell, 1967; Altenbach *et al.*, 1990; Greenhalgh *et al.*, 1991), and are distinctively different for each position. Some obvious qualitative conclusions can be drawn from these spectra without a detailed analysis. For C62, C140, and C316, there is a well-resolved contribution from an immobile component (labeled α), indicating structural rigidity in the corresponding cytoplasmic loop domain. As mentioned above, the spectrum at C240 has a dominant component of high mobility, suggesting a less structured environment, consistent with the high collision rate with diffusible reagents at this site.

The line shapes of I at C140, C240, and C316 are, within experimental error, the same in digitonin and lauryl maltoside, demonstrating that the protein conformation in these regions is similar in the two detergents. In contrast, the spectrum at C65 in digitonin has a small relative increase in resonance intensity in the low-field portion of the spectrum and an increase in the central line width compared to lauryl maltoside, differences most simply interpreted in terms of an increase in a motionally restricted population in digitonin. This is consistent with the more ordered interior of the digitonin micelle (Hong & Hubbell, 1973). A more subtle change of a similar nature may be seen at C62. However, less significance should be attached to this latter observation, since this mutant shows some variability in the EPR spectra between preparations. This may be due to a folding problem, since this mutant also has a much lower expression than the others, and has a slightly blue-shifted λ_{max} (Table I). In addition, this mutant appears to have more than one sulfhydryl modified by the spin-label, perhaps reflecting some degree of unfolding (Table II).

(C) Conformational Changes Associated with Bleaching. In order to study conformational changes which occur during the meta I to meta II transition, rhodopsin was solubilized in digitonin or lauryl maltoside (Konig *et al.*, 1989b). Figure 6A demonstrates that rhodopsin bleached in lauryl maltoside forms a photointermediate with a λ_{max} = 380 nm. Acidification of the bleached solution results in the formation of a 440-nm-absorbing protonated Schiff base, indicating that retinal is covalently bound to rhodopsin in the 380-nm absorption state (Matthews *et al.*, 1963). Furthermore, successive spectra taken at 2-min intervals (Figure 6B) show that the 380-nm absorbance decays to a 450-nm species, consistent with formation of the meta III photoproduct. This decay was inhibited by transducin, indicating that the 380-nm-absorbing species, like meta II, forms a stable complex with G_t in lauryl maltoside (Figure 6C). Taken together, these results indicate that meta II is the predominant initial species after bleaching in lauryl maltoside.

When digitonin-solubilized rhodopsin was bleached at 4 °C, a 480-nm-absorbing species consistent with meta I was formed (Figure 7A). The presence of transducin shifted meta I to meta II (Figure 7B). The binding of GMPPNP to the transducin–rhodopsin complex shifted the meta II species back to meta I, as a result of the dissociation of G_t. The ability of digitonin-solubilized rhodopsin to form meta II is dependent

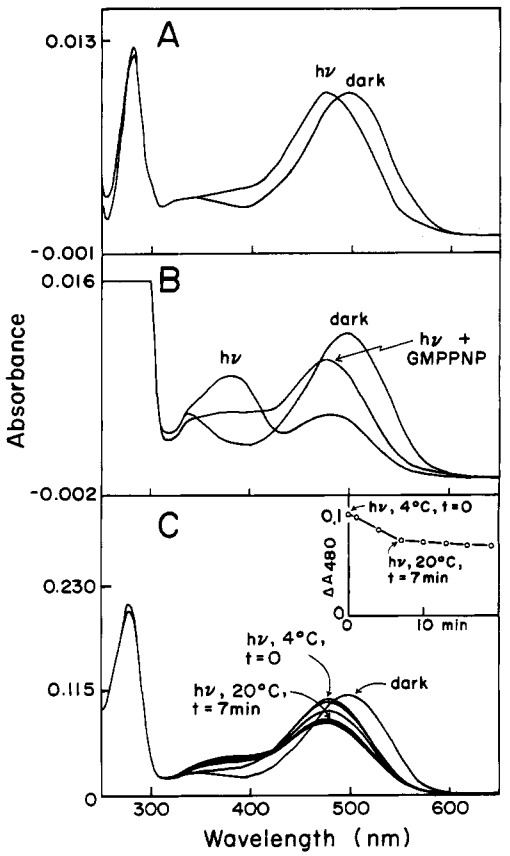

FIGURE 7: Bleaching of bovine rhodopsin in digitonin. (A) At 4 °C, the meta I intermediate is formed exclusively. (B) In the presence of transducin (1 μM), meta I is shifted to meta II. This is reversed after GMPPNP (10 μM) is added. (C) To inhibit meta II formation, ROS membranes were solubilized in lauryl maltoside, and the detergent was exchanged to digitonin during rhodopsin purification. Bleaching at 4 °C produces meta I (480 nm). Raising the temperature to 20 °C resulted in a 20% loss in the meta I species. After this initial loss in absorbance, no further change is seen.

on a lipid component which is copurified with the protein as was previously demonstrated (Schichi *et al.*, 1977). Solubilization in lauryl maltoside followed by detergent exchange into digitonin resulted in delipidation of the protein and an inability to form meta II. Figure 7C shows bleaching of delipidated rhodopsin solubilized in digitonin. Bleaching performed at 4 °C gave exclusively the meta I intermediate at pH 6. As the temperature was raised to 20 °C over a 7-min period, there was a 20% loss in absorbance at 480 nm. No further change in the 480-nm species was observed at 20 °C (see inset). Similar phenomena have been observed previously (Blazynski & Ostroy, 1981). Acid denaturation of the digitonin-solubilized sample indicated that loss of the 480-nm species was due to the formation of free retinal. Further illumination at 20 °C also produced free retinal (data not shown).

The above results demonstrate that the meta I or meta II state can be selectively produced by bleaching rhodopsin in either digitonin or lauryl maltoside, respectively. Thus, a comparison of the EPR spectra of bleached, spin-labeled rhodopsin in these detergents should reveal any conformational changes unique to either the meta I or the meta II states. Figure 8 compares EPR spectra of the labeled mutants at C140 and C316 in the dark and after bleaching, both in lauryl maltoside and in digitonin. At C140, bleaching in lauryl maltoside produces large changes in the low-field region, highly reproducible and well above the signal-to-noise ratio. At C316, bleaching also produces reproducible changes in lauryl

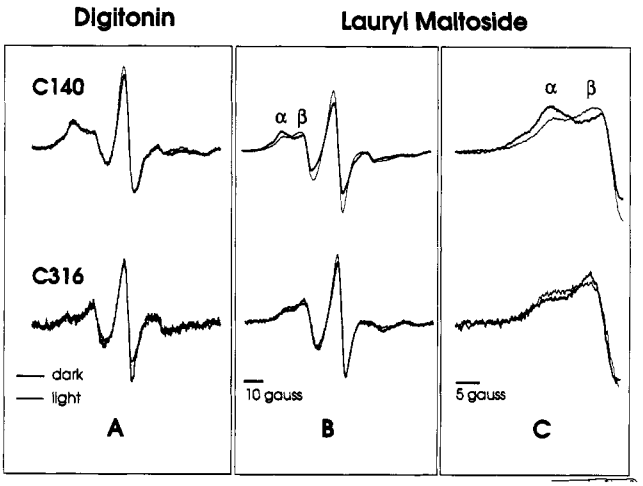

FIGURE 8: Light-induced EPR spectral changes in spin-labeled rhodopsin mutants. In (A) and (B), the spectra of labeled 140 and 316 are compared in the dark (thicker line) and light (thinner line) in both lauryl maltoside and digitonin. In (C), the low-field regions of the spectra in (B) are expanded to reveal more clearly the changes observed upon bleaching.

maltoside, although less than at C140. There is essentially no change in line shape at C62, C65, or C240 (not shown).

No significant changes are detected upon bleaching at any of these positions in digitonin. This important result supports the conclusion that the changes observed in lauryl maltoside are associated with the meta I to meta II transition.

It is important to note that derivatization of C140 and C316 with spin-label I did not affect the nature of the photoproducts, and meta I and meta II were the dominant photoproducts in digitonin and lauryl maltoside, respectively. This result indicates that modification at this position produces little perturbation of the structure, consistent with earlier results (Hoffman & Reichert, 1985).

DISCUSSION

Five mutants have been constructed with unique cysteines introduced into the cytoplasmic face of rhodopsin. All of the mutants bound 11-*cis*-retinal and gave UV–vis spectra similar to the wild-type rhodopsin. The mutants all gave a glycosylation pattern indicating that they were properly folded and transported to the cytoplasmic membrane. Furthermore, each of the mutants activated transducin. These results indicate that the structure of the mutants is similar to that of the WT protein.

The data obtained from the EPR spectra of the spin-labeled mutants generally support the model of rhodopsin shown in Figure 1 and add new structural information. The high mobility of a nitroxide at C240 and the high accessibility to collision with diffusible reagents suggest an extended, mobile loop around this site. This is consistent with the interhelical loop location shown in the structural model of Figure 1, the rapid proteolysis by a number of proteases, and the activity of transglutaminase toward this domain (Pober *et al.*, 1978). The Π values at positions C62, C65, C140, and C316 also suggest that these are solvent-exposed sites, consistent with the structural model, but the EPR line shapes show that they are much more ordered than the domain around C240.

The relative Π values for Crox and $Ni(AA)_2$ suggest a positive electrostatic potential around C62 and C65. This result is also consistent with the structural model of Figure 1, since there are four positive charges in the string 62–69.

It has been postulated that the palmitoylated sites at cysteines 322 and 323 anchor the polypeptide to the membrane,

thus defining a fourth cytoplasmic loop that would contain C316 (Karnick *et al.*, 1993). The palmitoylated cysteines at position 322 and 323 are absent in the mutants studied here. Nevertheless, the line shape of the spin-label at position 316 indicates a highly ordered domain, suggesting that the putative 322, 323 anchor is not necessary for a structured domain.

The EPR line shapes for the nitroxides at positions C140 and C316 are complex, consisting of at least two spectral components (Figures 5 and 8). While it is possible for apparent multicomponent line shapes to arise from a single population with anisotropic motion (Meirovich & Freed, 1984), spectra similar to those for I at C140 and C316 have been previously observed in other spin-labeled proteins and, in the case of hemoglobin, have been demonstrated to be due to two conformations of the spin-label (Ogawa & McConnell, 1967; Moffat, 1971). In one conformer, the nitroxide makes direct contacts with nearby side chains and is relatively immobile. In the other, it is free to move by rotation about internal bonds. The consistent appearance of two-component spectra at many different sites in a number of labeled proteins with nitroxides of different structure (Todd *et al.*, 1989; Greenhalgh *et al.*, 1991; Altenbach *et al.*, 1990) suggests that this may be a general situation, and is the most likely interpretation of the spectra arising from 140 and 316 of rhodopsin.

Reproducible light-induced changes are observed in the EPR line shapes of (I) at 140 and 316 in lauryl maltoside, but not in digitonin. Since meta II is formed in lauryl maltoside but not in digitonin, these changes are assumed to be associated with meta II formation. As can be seen in Figure 8, the spectral change reflects a change in the relative amount of the two nitroxide populations, and it must arise from relative movement of the nitroxide and the interaction site(s) that distinguish-(es) the two populations. It is not possible to deduce the magnitude of such a movement from these data alone, but it is likely to be small considering the small spectral change. Similar changes in the EPR spectra of spin-labeled hemoglobin were observed upon changes in oxygenation, and resulted from local protein movements of no more than a few angstroms. It is interesting to note that the estimated helix displacement in bacteriorhodopsin during the photocycle amounts to about 2 Å (Subramaniam *et al.*, 1993).

Cysteines 140 and 316 are located at the cytoplasmic termination of helices C and G, respectively (see Figure 1). These helices contain the protonated Schiff bases and its Glu113 counterion, respectively. Upon meta II formation, this salt bridge has been broken and removes an important structural constraint on the two helices. This event may permit thermal motion of the helices, resulting in the changes detected by the nitroxides at C140 and C316. Since meta II is the species which interacts with transducin, and the cytoplasmic surface of rhodopsin is known to contain the transducin binding site, it is significant that a detectable change occurs in this region when the protein enters the meta II state. The conformational changes are presumably a part of the mechanism by which the transducin binding site is exposed.

The third cytoplasmic loop (E–F loop) containing C240 is also believed to interact with transducin in the meta II state (Konig *et al.*, 1989a; Franke *et al.*, 1990), but no change is detected by the spin-label at this site upon bleaching. However, the high degree of mobility of the nitroxide at site C240 implies that it has little or no direct interaction with the protein other than being tethered. Thus, it is expected to have little sensitivity to conformational changes.

Light-induced spectral changes are not detected by spin-label I at C62 or C65 in either lauryl maltoside or digitonin. This is significant, since nitroxides at these positions have strong interactions with the protein, and are expected to have high sensitivity to changes in structure.

In conclusion, the studies presented above represent the first application of the site-directed spin-labeling technique to rhodopsin, and offer a new line of evidence regarding the structure and conformational changes in the protein. Residues C62, C65, C140, C240, and C316 are all solvent-exposed, consistent with the assignment of the cytoplasmic loops predicted from hydrophobic analysis. Sites C62, C65, C140, and C316 are located in highly ordered environments, while C240 appears to be in a mobile, less structured domain. Finally, meta II formation results in conformational changes in the cytoplasmic surface of the protein. This result is complemented by a time-resolved EPR study in the native disk membrane which shows that the conformational change at C140 appears with a time constant and activation energy consistent with the appearance of the meta II optical signal (Farabakhsh *et al.*, 1993). Future work with site-directed spin-labeling will define the helical borders of rhodopsin, determine the complete topology of the conformational changes, and allow examination of the rhodopsin–transducin interaction.

ACKNOWLEDGMENT

Thanks to Dr. Z. Lu, Dr. D. Farrens, and Dr. F. Davidson for helpful suggestions and critical reading of the manuscript. Special thanks to J. Carlin for her exceptional help in typing the manuscript.

REFERENCES

Altenbach, C., Flitsch, S. L., Khorana, H. G., & Hubbell, W. L. (1989) *Biochemistry 28*, 7806–7812.

Altenbach, C., Marti, T., Khorana, H. G., & Hubbell, W. L. (1990) *Science 248*, 1088–1092.

Baehr, W., Morita, E. A., Swanson, R. J., & Applebury, M. L. (1982) *J. Biol. Chem. 257*, 6451–6460.

Blazynski, C., & Ostroy, S. E. (1981) *Vision Res. 21*, 833–841.

Emeis, D., Kuhn, H., Reichert, J., & Hofmann, K. P. (1982) *FEBS Lett. 143*, 29.

Farahbakhsh, Z. T., Altenbach, C., & Hubbell, W. L. (1992) *Photochem. Photobiol. 56*, 1019–1033.

Farahbakhsh, Z. T., Hideg, K., & Hubbell, W. (1993) *Science* (in press).

Ferretti, L., Karnik, S. S., Khorana, H. G., Nassal, M., & Oprian, D. D. (1986) *Proc. Natl. Acad. Sci. U.S.A. 83*, 599–603.

Findlay, J. B. C., Barclay, P. L., Brett, M., Davidson, M., Pappin, D. S. C., & Tompson, P. (1984) *Vision Res. 24*, 1301–1308.

Franke, R. R., Konig, B., Sakmar, T. P., Khorana, H. G., & Hofmann, K. P. (1990) *Science 250*, 123–125.

Franke, R. R., Sakmar, T. P., Graham, R. M., & Khorana, H. G. (1992) *J. Biol. Chem. 267*, 14767–14774.

Fung, B. K. K., Hurley, J. B., & Stryer (1981) *Proc. Natl. Acad. Sci. U.S.A. 78*, 152–156.

Greenhalgh, D. A., Subramaniam, S., Alexiev, U., Otto, H., Heyn, M. P., & Khorana, H. G. (1992) *J. Biol. Chem. 267*, 25734–25738.

Hargrave, P. A., McDowell, J. H., Curtis, D. R., Wang, J. K., Juszczak, E., Fong, S.-L., Mohana Rao, J. K., & Argos, P. (1983) *Biophys. Struct. Mech. 9*, 235–244.

Henderson, R., Baldwin, J. M., Ceska, T. A., Zemlin, F., Beckmann, E., & Downing, K. H. (1990) *J. Mol. Biol. 213*, 899–929.

Hoffman, K. P., & Reichert, J. (1985) *J. Biol. Chem. 260*, 7990–7995.

Hong, K., & Hubbell, W. L. (1973) *Biochemistry 12*, 4517–4523.

Hubbell, W. L., & Altenbach, C. (1993) in *Membrane Protein Structure; Experimental Approaches* (White, S., Ed.) Oxford

Press, New York.
Hubbell, W. L., Froncisz, W., & Hyde, J. S. (1987) *Rev. Sci. Instrum. 58*, 1879–1886.
Karnik, S. S., & Khorana, H. G. (1990) *J. Biol. Chem. 265*, 17520–17524.
Karnik, S. S., Sakmar, T. P., Chen, H.-B., & Khorana, H. G. (1988) *Proc. Natl. Acad. Sci. U.S.A. 85*, 8459–8463.
Karnik, S. S., Ridge, K. D., Bhattacharya, S., & Khorana, H. G. (1993) *Proc. Natl. Acad. Sci. U.S.A. 90*, 40–44.
Konig, B., Arendt, A., McDowell, J. H., Kahlert, M., Hargrave, R. A., & Hofmann, K. P. (1989a) *Proc. Natl. Acad. Sci. U.S.A. 86*, 6878–6882.
Konig, B., Hofmann, K. P., & Wolfe, W. (1989b) *FEBS Lett. 257*, 163–166.
Kuhn, H. (1984) *Prog. Retinal Res. 3*, 123–136.
Matthews, R. G., Hubbard, R., Brown, P. K., & Wald, G. (1963) *J. Gen. Phys. 47*, 215–240.
Meirovitch, E., & Freed, J. H. (1984) *J. Phys. Chem. 88*, 4995–5004.
Moffat, J. K. (1971) *J. Mol. Biol. 55*, 135–146.
Molday, R. S., & Mackenzie, D. (1983) *Biochemistry 22*, 653–680.
Nakayama, T. A., & Khorana, H. G. (1991) *J. Biol. Chem. 266*, 4269–4275.
Nathans, J. (1990) *Biochemistry 29*, 9746–9752.
Nathans, J., & Hogness, D. S. (1983) *Cell 34*, 807–814.
Ogawa, S., & McConnell, H. M. (1967) *Proc. Natl. Acad. Sci. U.S.A. 58*, 401–405.
Oprian, D. D., Molday, R. S., Kaufman, R. J., & Khorana, H. G. (1987) *Proc. Natl. Acad. Sci. U.S.A. 84*, 8874–8878.
Ovchinnikov, Y. A., Abdulaev, N. G., Feigina, M. Y., Artamonov, I. D., Zolotarev, A. S., Kostina, M. B., Bogachuk, A. S., Miroshnikov, A. I., Martinov, V. I., & Kudelin, A. B. (1982) *Bioorg. Khim. 8*, 1011–1014.
Papermaster, D. S. (1982) *Methods Enzymol. 81*, 48–52.
Pober, J. S., Iwanij, V., Reich, E., & Stryer, L. (1978) *Biochemistry 17*, 2163–2168.
Sakmar, T. P., Franke, R. R., & Khorana, H. G. (1989) *Proc. Natl. Acad. Sci. U.S.A. 88*, 3079–3083.
Shichi, H., Kawamura, S., Muellenberg, C. G., & Yoshizawa (1977) *Biochemistry 16*, 5376–5381.
Subramaniam, S., Gerstein, M., Oesterhelt, D., & Henderson, R. (1993) *EMBO J. 12*, 1–8.
Todd, A. P., Cong, J., Levinthal, F., Levinthal, C., & Hubbell, W. L. (1989) *Proteins: Struct., Funct., Genet. 6*, 294–305.
Wald, G. (1968) *Nature 213*, 800–807.
Wessling-Resnick, M., & Johnson, G. L. (1987) *J. Biol. Chem. 262*, 3697–3705.
Zhukovsky, E. A., & Oprian, D. D. (1989) *Science 246*, 928–930.